Smart Structures and Systems, *Vol. 24, No. 3 (2019) 333-343*
DOI: https://doi.org/10.12989/sss.2019.24.3.333

Energy harvesting from piezoelectric strips attached to systems under random vibrations

Francesco Trentadue[1], Giuseppe Quaranta[*2], Claudio Maruccio[3] and Giuseppe C. Marano[4]

[1]*Department of Civil Engineering and Architecture, Technical University of Bari, via Orabona 4, 70125 Bari, Italy*
[2]*Department of Structural and Geotechnical Engineering, Sapienza University of Rome, via Eudossiana 18, 00184 Rome, Italy*
[3]*Department of Innovation Engineering, University of Salento, via Monteroni, 73100 Lecce, Italy*
[4]*Department of Structural, Geotechnical and Building Engineering, Politecnico di Torino, corso Duca degli Abruzzi 24, 10129 Torino, Italy*

(Received August 23, 2018, Revised April 26, 2019, Accepted July 3, 2019)

Abstract. The possibility of adopting vibration-powered wireless nodes has been largely investigated in the last years. Among the available technologies based on the piezoelectric effect, the most common ones consist of a vibrating beam covered by electroactive layers. Another energy harvesting strategy is based on the use of piezoelectric strips attached to a hosting structure subjected to dynamic loads. The hosting structure, for example, can be the system to be equipped with wireless nodes. Such strategy has received few attentions so far and no analytical studies have been presented yet. Hence, the original contribution of the present paper is concerned with the development of analytical solutions for the electrodynamic analysis and design of piezoelectric polymeric strips attached to relatively large linear elastic structural systems subjected to random vibrations at the base. Specifically, it is assumed that the dynamics of the hosting structure is dominated by the fundamental vibration mode only, and thus it is reduced to a linear elastic single-degree-of-freedom system. On the other hand, the random excitation at the base of the hosting structure is simulated by filtering a white Gaussian noise through a linear second-order filter. The electromechanical force exerted by the polymeric strip is negligible compared with other forces generated by the large hosting structure to which it is attached. By assuming a simplified electrical interface, useful new exact analytical expressions are derived to assess the generated electric power and the integrity of the harvester as well as to facilitate its optimum design.

Keywords: electrospun piezoelectric nanofibers; energy harvesting; random vibrations; smart structures; structural monitoring

1. Introduction

A critical issue in smart structures is the way by which the electric energy for operating a wireless node is provided. Amongst the available technologies, harnessing the energy from ambient vibrations is especially promising for civil engineering applications (Hancke *et al*. 2013) and, in this field, piezoelectric devices have been largely studied in the past years.

For instance, Elvin *et al*. (2006) estimated numerically the electrical energy that can be converted through the piezoelectric effect for three dynamic loading conditions, i.e. traffic loads on a bridge, wind-induced response of buildings and seismic accelerations. Ali *et al*. (2011) considered a simplified highway bridge model subjected to a point load moving on it in order to estimate analytically the energy generated from a piezoelectric harvester under the passage of a single vehicle. Experimental results and finite element analyses of piezoelectric energy harvesters for highway bridges have been also presented in (Peigney and Siegert 2013, Zhang *et al*. 2014, Cahill *et al*. 2016). Maruccio *et al*. (2016) have studied the feasibility of piezoelectric energy harvesters for self-powered wireless sensor nodes intended for the structural health monitoring of a cable-stayed bridge. Piezoelectric energy harvesting from train-induced bridge response is studied by Cahill *et al*. (2014) whereas a novel piezoelectric energy harvester to be installed into high-rise buildings has been illustrated in (Xie *et al*. 2013, 2015). Cahill *et al*. (2018) proposed a novel approach in which piezoelectric energy harvesting devices are employed for damage detection in pipelines that convey fluids.

While numerical modeling and computational approaches can provide an accurate prediction of the electromechanical response of energy harvesting devices (Maruccio *et al*. 2018, Kefal *et al*. 2019), analytical solutions (even if based on simplified models) can be very useful at the preliminary stage because they require less elaboration time and can give immediate information for the optimum design. Several interesting results have been obtained in this regard, either under harmonic loads or random vibrations.

Generally, the random vibration theory is more appropriate to study the electromechanical response of energy harvesters subjected to uncertain excitations. Within this framework, Adhikari *et al*. (2009) estimated analytically the average power generated from a piezoelectric vibration-based energy harvester. In doing so, they considered a linear elastic single-degree-of-freedom (SDOF) vibration energy harvesting system under white

∗Corresponding author, Assistant Professor
E-mail: giuseppe.quaranta@uniroma1.it

ISSN: 1738-1584 (Print), 1738-1991 (Online)

Gaussian noise (WGN) whereas two electrical interfaces have been taken into account, namely a circuit including a resistor with or without an inductor. For these electrodynamic configurations, Adhikari *et al*. (2016) also obtained closed-form expressions to estimate level crossing of the voltage, response voltage peaks above certain level and fractional time of the voltage response above a certain level. Another analytical study has been presented by Zhao and Erturk (2012), who investigated the electroelastic response under broadband random vibrations of a cantilever bimorph with a resistor box connected to the electrode terminals.

Recently, a more complete probabilistic characterization of the output energy – in terms of mean and standard deviation – has been obtained by the present authors for an elastic piezoelectric bimorph under amplitude-modulated and filtered WGN considering a resistive electrical load (Quaranta *et al*. 2017, 2018). Useful analytical results have been also obtained by extending the random vibration analysis to nonlinear electrodynamic problems. For example, the optimum design of a nonlinear SDOF energy harvester excited by WGN and connected to a resistor is performed in (He and Daqaq 2016).

In this perspective, the present paper aims at contributing to the analytical study of energy harvesters under uncertain dynamic loads. Herein, the focus is on electroactive polymeric strips attached to relatively large linear elastic hosting systems subjected to random vibrations at the base. For instance, the hosting structure might be the system to be equipped with vibrations-powered wireless nodes. Despite its potential practical applications, such energy harvesting strategy has received few attentions and no analytical results are available yet. Specifically, the dynamics of the hosting structure is reduced to a linear elastic SDOF system under the assumption that it is dominated by a single fundamental mode of vibration. The uncertain base vibrations are modeled by filtering a white Gaussian noise through a linear second-order filter. As regards the energy harvesting device, it is considered a piezoelectric polymeric strip attached to this hosting structure whereas a simplified electrical interface consisting of a resistive electrical load only is adopted in agreement with previous studies. The electromechanical force exerted by the polymeric strip is negligible compared with other forces generated by the hosting structure to which it is attached. Within this framework, exact closed-form solutions are derived to study and optimize the electromechanical response of the piezoelectric device and to assess its integrity. Numerical results for an electroactive polymeric strip made of electrospun PVDF nanofibers (Persano *et al*. 2013, 2014, Ico *et al*. 2016) are finally presented and discussed.

2. Stochastic analysis of piezoelectric strip attached to elastic structural system

2.1 Energy harvesting strategy

Several piezoelectric energy harvesting strategies usually exploit the response of electroactive layers bonded to a vibrating element, e.g., an unimorph or bimorph cantilever beam subjected to dynamic loads. An alternative strategy consists of thin piezoelectric strips attached to a hosting structural system subjected to dynamic loads. For instance, Cahill *et al*. (2014) considered an energy harvesting system based on an adhesive patch bonded to a bridge for generating electric power under the passage of trains, and they state that this strategy might be potentially effective for structural monitoring applications. As a further example in the field of civil engineering, Fig. 1 illustrates a possible application of this strategy for buildings.

For the purposes of the present study, the hosting structure can be any linear elastic civil or mechanical system under base vibrations (e.g., a system to be equipped with wireless nodes) whose dimensions and inertia are much larger than those of typical piezoelectric strips. Because of the large dimensions of the hosting structure, in order to generate as much electrical energy as possible even under low excitation levels, the piezoelectric strip is designed in order to operate according to the 3-1 mode in such a way to maximize the electrode area. Moreover, although the following theoretical results can apply to any piezoelectric materials, manufacturing issues and expected deformation demands make polymeric piezoelectric materials especially suitable for such kind of potential applications. Finally, a perfect bond will be assumed between the piezoelectric strip and the hosting structure.

2.2 Electromechanical modeling of the piezoelectric strip

A thin electroactive polymeric strip operating in the 3-1 mode is considered (see Fig. 2). Taking into account material properties and device configuration, it is assumed for sake of simplicity that the piezoelectric strain constants d_{31} and d_{32} are equal each other. Furthermore, the only non-null stress components in this analysis are T_1 and T_2 whereas the strain component S_2 is null and the only non-null electric field and electric displacement components are

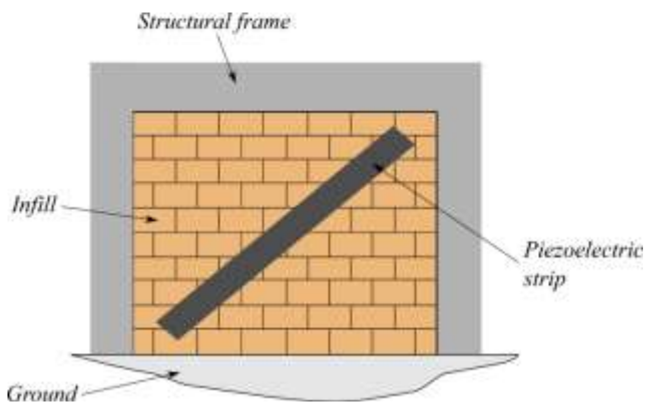

Fig. 1 Piezoelectric thin strip attached to a structural building frame

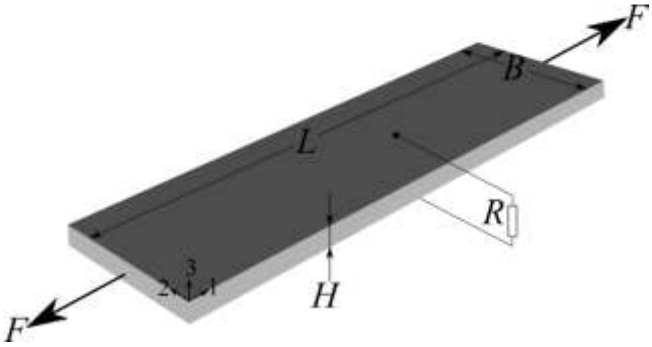

Fig. 2 Thin piezoelectric strip operating in the 3-1 mode

E_3 and D_3, respectively. More precise assumptions can be adopted, but preliminary numerical analyses have confirmed that these hypotheses lead to accurate results for the scopes of the present work.

Under the above assumptions, the constitutive equations of the piezoelectric element read

$$\begin{cases} S_1 = \dfrac{1}{E_m}(T_1 - \nu T_2) + d_{31}E_3 \\ 0 = \dfrac{1}{E_m}(T_2 - \nu T_1) + d_{31}E_3 \\ D_3 = d_{31}(T_1 + T_2) + \epsilon_{33}^T E_3 \end{cases} \tag{1}$$

Herein, E_m and ν are Young modulus and Poisson ratio of the piezoelectric material, respectively, whereas ϵ_{33}^T is its permittivity. Eq. (1) can also be written as

$$\begin{cases} T_1 = \dfrac{E_m}{1-\nu^2}(S_1 - (1+\nu)d_{31}E_3) \\ T_2 = \dfrac{E_m}{1-\nu^2}(\nu S_1 - (1+\nu)d_{31}E_3) \\ D_3 = d_{31}\dfrac{E_m}{1-\nu}S_1 + \left(\epsilon_{33}^T - 2d_{31}^2\dfrac{E_m}{1-\nu}\right)E_3 \end{cases} \tag{2}$$

Now, let $A_F = BH$ be the area where the force F applies, q the electric charge that accumulates on the electrodes area $A_{el} = BL$, v the electric potential and y the relative displacement component. Then, the following relationships apply

$$E_3 = -\frac{v}{H}, \qquad S_1 = \frac{y}{L}, \qquad D_3 = \frac{q}{A_{el}}, \qquad T_1 = \frac{F}{A_F} \tag{3}$$

As a consequence, from Eqs. (2) and (3) is obtained

$$\begin{cases} F = Ky - \Theta v \\ q = -Cv + \Theta y \end{cases} \tag{4}$$

where the adopted constants are

$$C = \left(\epsilon_{33}^T - \frac{2d_{31}^2 E_m}{1-\nu}\right)\frac{BL}{H} \tag{5a}$$

$$K = \left(\frac{E_m}{1-\nu^2}\right)\frac{BH}{L} \tag{5b}$$

$$\Theta = \frac{E_m B d_{31}}{1-\nu} \tag{5c}$$

Herein, C, K and Θ are capacitance, elastic stiffness and piezoelectric coupling factor of the piezoelectric insert operating in the 3-1 mode, respectively.

The accurate modeling of the electrical circuit is outside the scopes of this work. Without loss of generality and in agreement with the majority of the previous studies in this field, it is assumed that the two opposite faces of the piezoelectric strip with the largest area are connected to a resistive electrical load as shown Fig. 2, see for instance (Elvin *et al.* 2006, Adhikari *et al.* 2009, Ali *et al.* 2011, Rhimi and Lajnef 2012, Cahill *et al.* 2014, Zhang *et al.* 2014, Xiao *et al.* 2015, Adhikari *et al.* 2016, Cahill *et al.* 2016, Karimi *et al.* 2016, Maruccio *et al.* 2016, Yang *et al.* 2017, Quaranta *et al.* 2018). It has been pointed out, however, that resistive loads may also realistically simulate some power-management circuits (Halvorsen 2008).

By introducing the time variable t, the final electrodynamic equation of the harvester can be written as follows

$$CR\dot{v}(t) + v(t) - \Theta R\dot{y}(t) = 0 \tag{6}$$

where R is the resistive electric load and the dot indicates the time derivative. Note that the numerical value of R can be defined to take into account the external load resistance and the internal resistance (in such a case, R refers to a total or equivalent resistance value), see for instance (Xiao *et al.* 2015).

2.3 Random excitation model

In the present work, the hosting structural system is subjected to a random accelerations $\ddot{x}_b(t)$ at the base for a given duration T. A consolidated and effective stochastic modeling for random loads characterized by non-uniform frequency contents is obtained by filtering a WGN. Specifically, the random acceleration is here modeled by filtering the WGN through a second-order linear (Kanai-Tajimi) filter, see for instance (Marano *et al.* 2009, Greco and Trentadue 2013). So doing, $\ddot{x}_b(t)$ is given by (see Fig. 3)

$$\ddot{x}_b(t) = -2\xi_f\omega_f\dot{x}_f(t) - \omega_f^2 x_f(t) \tag{7}$$

where $x_f(t)$ is the solution of the following stochastic equation under zero initial conditions

$$\ddot{x}_f(t) + 2\xi_f\omega_f\dot{x}_f(t) + \omega_f^2 x_f(t) = -\varphi(t)w(t) \tag{8}$$

Herein, ω_f and ξ_f are the filter parameters (ω_f is the filter circular frequency while ξ_f is the filter damping, with $0 \le \xi_f \le 1$). Furthermore, $\varphi(t)$ is a deterministic function that modulates the intensity of the zero-mean WGN $w(t)$ within the time window $[0, T]$. Herein, the rectangular box modulation function $\varphi(t)$ is assumed

$$\varphi(t) = \begin{cases} 1 & \text{if } 0 \le t \le T \\ 0 & \text{otherwise} \end{cases} \tag{9}$$

It should be remarked that no special restrictions are imposed to the length of the time window T. The solution of Eqs. (7) and (8) can be conveniently posed in form of convolution product, thus obtaining

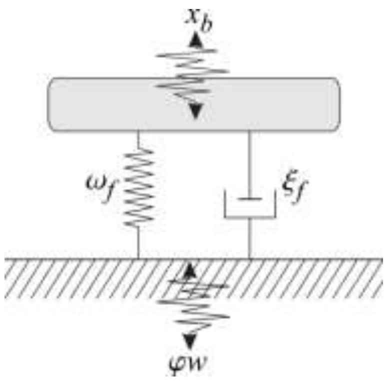

Fig. 3 Numerical modeling of the random dynamic excitation

$$\ddot{x}_b(t) = \left[h_{\ddot{x}_b} * w_\varphi\right](t) = \int_{-\infty}^{\infty} h_{\ddot{x}_b}(t-\tau)\, w_\varphi(\tau) d\tau \tag{10}$$

where $w_\varphi(\tau) = \varphi(\tau) w(\tau)$ and

$$h_{\ddot{x}_b}(\theta) = \begin{cases} -\dfrac{e^{-\xi_f \omega_f \theta}}{\sqrt{1-\xi_f^2}}\left(\left(1-2\xi_f^2\right)\omega_f \sin\left(\tilde{\omega}_f \theta\right) + 2\xi_f \tilde{\omega}_f \cos\left(\tilde{\omega}_f \theta\right)\right) & \text{if } \theta \geq 0 \\ 0 & \text{if } \theta < 0 \end{cases} \tag{11}$$

with $\tilde{\omega}_f = \omega_f\left(1-\xi_f^2\right)^{\frac{1}{2}}$. A pure WGN-type base acceleration can be obtained by assuming $\ddot{x}_b(t) = -w_\varphi(t)$.

2.4 Response of the piezoelectric energy harvester

A linear elastic and classically damped hosting structure subjected to the random acceleration $\ddot{x}_b(t)$ at the base is considered. It is assumed that the dynamics of the hosting structure is dominated by the fundamental mode of vibration. Under this assumption, the hosting structure can be analyzed in the modal space by means of a linear elastic SDOF system (see Fig. 4). The relative modal displacement of the hosting system is denoted as $x(t)$ whereas ω_s and ξ_s are the natural circular frequency and damping ratio, respectively (with $0 \leq \xi_s \leq 1$).

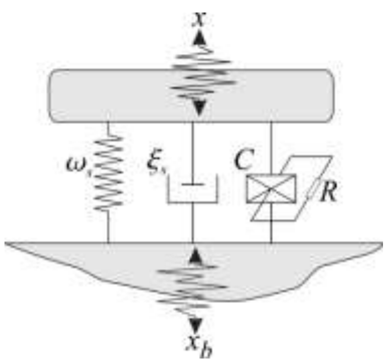

Fig. 4 Numerical modeling of the linear elastic structure with a piezoelectric insert (note that the piezoelectric insert is designed to operate in the 3-1 mode)

Under the hypothesis of a perfect bond between the piezoelectric strip and the hosting structure, the displacement response of the piezoelectric insert $y(t)$ can be generally expressed as $y(t) = \alpha x(t)$. The coefficient α is here introduced to reflect that the response of the hosting system is analyzed in the modal space while the real displacement response of the piezoelectric insert is required into Eq. (6), but also to eventually take into account other aspects, such as a non-zero angle between the main axis of the piezoelectric strip and the modal coordinate of the hosting structure. Having assumed that dimensions and inertia of the hosting structure are much larger than those of the piezoelectric strip, it is evident that the electromechanical force developed by the electroactive polymeric insert is certainly negligible with respect to inertial, elastic and dissipative forces generated by the structural system to which it is attached. The response of the piezoelectric energy harvester is then defined by the following equations

$$\ddot{x}(t) + 2\xi_s \omega_s \dot{x}(t) + \omega_s^2 x(t) = -\Lambda \ddot{x}_b(t) \tag{12}$$

$$\dot{v}(t) + \frac{1}{RC} v(t) - \frac{\alpha \Theta}{C} \dot{x}(t) = 0 \tag{13}$$

where Λ is the modal participation factor (please note that $y(t)$ has been replaced with $\alpha x(t)$ in Eq. (13) as explained before). Once again, it is remarked that the lack of the electromechanical coupling term in Eq. (12) is due to the fact that the force exerted by the piezoelectric strip has no effects on the dynamics of the hosting structure. It is also highlighted that these equations are valid under the assumption of linear elastic behavior for the hosting structural system. However, the following results can be still applied when the hosting structural system exhibits a nonlinear response by performing a statistical linearization. The case of nonlinear hosting systems will be not addressed explicitly in the present work, but the interested reader can refer to (Roberts and Spanos 1990) for useful information about equivalent linearization techniques under random vibrations. Since the electromechanical force generated by the piezoelectric strip is negligible compared with the other forces generated by the hosting structure, the equations describing the response of the whole system (structural system and piezoelectric insert) can be decoupled. So doing, the solution is obtained by sequentially solving the filter's equations given by Eqs. (7) and (8), the dynamic motion equation in Eq. (12) and, finally, Eq. (13). In order to solve Eq. (12), it is first determined the response function $\bar{h}_{\dot{x}}(\theta)$ of the relative modal velocity of the hosting system to an impulse of acceleration at the base, which reads:

$$\bar{h}_{\dot{x}}(\theta) = \begin{cases} \Lambda e^{-\xi_s \omega_s \theta}\left(\left(\dfrac{\xi_s \sin(\tilde{\omega}_s \theta)}{\sqrt{1-\xi_s^2}}\right) - \cos(\tilde{\omega}_s \theta)\right) & \text{if } \theta \geq 0 \\ 0 & \text{if } \theta < 0 \end{cases} \tag{14}$$

where $\tilde{\omega}_s = \omega_s(1-\xi_s^2)^{\frac{1}{2}}$. Once the filter's equation is solved through Eqs. (10) and (11), the relative modal velocity of the system $\dot{x}(t)$ is determined by resorting to the associative property of the convolution product, thus obtaining

$$
\begin{aligned}
\dot{x}(t) &= \left[\bar{h}_{\dot{x}} * \ddot{x}_b\right](t) \\
&= \left[\bar{h}_{\dot{x}} * \left[h_{\ddot{x}_b} * w_\varphi\right]\right](t) \\
&= \left[\left[\bar{h}_{\dot{x}} * h_{\ddot{x}_b}\right] * w_\varphi\right](t) \\
&= \left[h_{\dot{x}} * w_\varphi\right](t)
\end{aligned}
\tag{15}
$$

where $h_{\dot{x}}(t)$ is the relative modal velocity response function of the hosting system to an impulse of WGN applied to the filter. Clearly, the velocity response function of the piezoelectric strip to an impulse of WGN applied to the filter is $h_{\dot{y}}(t) = \alpha h_{\dot{x}}(t)$ and it can be found that

$$
h_{\dot{y}}(\theta) = \begin{cases} \mathrm{e}^{-\xi_f \omega_f \theta}\left(-c\cos(\widetilde{\omega}_f\theta) + s_f \sin(\widetilde{\omega}_f\theta)\right) & \\ +\mathrm{e}^{-\xi_s \omega_s \theta}\left(c\cos(\widetilde{\omega}_s\theta) + s_s \sin(\widetilde{\omega}_s\theta)\right) & \text{if } \theta \geq 0 \\ 0 & \text{if } \theta < 0 \end{cases} .
\tag{16}
$$

where the expressions for the constants c, s_f and s_s are

$$
c = \frac{\alpha\Lambda\omega_f^2\left(4\xi_f\omega_f\xi_s\omega_s - \left(4\xi_f^2 - 1\right)\omega_s^2 - \omega_f^2\right)}{\Delta}
\tag{17a}
$$

$$
\begin{aligned}
s_f &= \frac{-\alpha\Lambda\omega_f^2\left(2\left(1 - 2\xi_f^2\right)\omega_f\xi_s\omega_s\right)}{\Delta\sqrt{1 - \xi_f^2}} \\
&+ \frac{-\alpha\Lambda\omega_f^2\left(\xi_f\left(4\xi_f^2 - 3\right)\omega_s^2 + \xi_f\omega_f^2\right)}{\Delta\sqrt{1 - \xi_f^2}}
\end{aligned}
\tag{17b}
$$

$$
\begin{aligned}
s_s &= \frac{\alpha\Lambda\omega_f\left(-2\xi_f\omega_s\left(\omega_s^2 + 2\omega_f^2\xi_s^2\right)\right)}{\Delta\sqrt{1 - \xi_s^2}} \\
&+ \frac{\alpha\Lambda\omega_f\left(\omega_f\xi_s\left(\left(4\xi_f^2 + 1\right)\omega_s^2 + \omega_f^2\right)\right)}{\Delta\sqrt{1 - \xi_s^2}}
\end{aligned}
\tag{17c}
$$

in which

$$
\begin{aligned}
\Delta = &\left(\left(\xi_f\omega_f - \xi_s\omega_s\right)^2 + \left(\widetilde{\omega}_f - \widetilde{\omega}_s\right)^2\right) \\
&\left(\left(\xi_f\omega_f - \xi_s\omega_s\right)^2 + \left(\widetilde{\omega}_f + \widetilde{\omega}_s\right)^2\right)
\end{aligned}
\tag{18}
$$

The voltage response function $\bar{h}_v(\theta)$ to an impulse of velocity of the piezoelectric strip is

$$
\bar{h}_v(\theta) = \begin{cases} \dfrac{\Theta}{C}\mathrm{e}^{-\frac{\Theta}{CR}} & \text{if } \theta \geq 0 \\ 0 & \text{if } \theta < 0 \end{cases}
\tag{19}
$$

whereas, by applying the associative property of the convolution product, it is found

$$
\begin{aligned}
v(t) &= \left[\bar{h}_v * \dot{y}\right](t) \\
&= \left[\bar{h}_v * \left[h_{\dot{y}} * w_\varphi\right]\right](t) \\
&= \left[\left[\bar{h}_v * h_{\dot{y}}\right] * w_\varphi\right](t) \\
&= \left[h_v * w_\varphi\right](t)
\end{aligned}
\tag{20}
$$

Herein, $h_v(\theta)$ is the voltage response to an impulse of WGN applied to the filter

$$
h_v(\theta) = \begin{cases} r\mathrm{e}^{-\frac{\theta}{CR}} & \\ +\mathrm{e}^{-\xi_f\omega_f\theta}\left(a_f\cos(\widetilde{\omega}_f\theta) + b_f\sin(\widetilde{\omega}_f\theta)\right) & \\ +\mathrm{e}^{-\xi_s\omega_s\theta}\left(a_s\cos(\widetilde{\omega}_s\theta) + b_s\sin(\widetilde{\omega}_s\theta)\right) & \text{if } \theta \geq 0 \\ 0 & \text{if } \theta < 0 \end{cases}
\tag{21}
$$

where the constants r, a_f, b_f, a_s and b_s are

$$
\begin{aligned}
r = -&\frac{\alpha\Lambda CR^2\Theta\omega_f\left(2\xi_f - CR\omega_f\right)}{\left(CR\omega_f\left(CR\omega_f - 2\xi_f\right) + 1\right)} \\
&\frac{1}{\left(CR\omega_s(CR\omega_s - 2\xi_s) + 1\right)}
\end{aligned}
\tag{22a}
$$

$$
a_f = \frac{R\Theta\left(c\left(1 - CR\xi_f\omega_f\right) - s_f CR\widetilde{\omega}_f\right)}{C^2R^2\widetilde{\omega}_f^2 + \left(CR\xi_f\omega_f - 1\right)^2}
\tag{22b}
$$

$$
b_f = \frac{R\Theta\left(s_f\left(1 - CR\xi_f\omega_f\right) + cCR\widetilde{\omega}_f\right)}{C^2R^2\widetilde{\omega}_f^2 + \left(CR\xi_f\omega_f - 1\right)^2}
\tag{22c}
$$

$$
a_s = -\frac{R\Theta(c(1 - CR\xi_s\omega_s) + s_s CR\widetilde{\omega}_s)}{C^2R^2\widetilde{\omega}_s^2 + (CR\xi_s\omega_s - 1)^2}
\tag{22d}
$$

$$
b_s = \frac{R\Theta(s_s(1 - CR\xi_s\omega_s) - cCR\widetilde{\omega}_s)}{C^2R^2\widetilde{\omega}_s^2 + (CR\xi_s\omega_s - 1)^2}
\tag{22e}
$$

and the constants c, s_f and s_s are given by Eq. (17).

The expected value of the power W after a time T is

$$
\mathrm{E}[W(T)] = \frac{\mathrm{E}[v^2(T)]}{R} = \frac{2\pi S_0}{R}\int_0^T h_v^2(t)\mathrm{d}t
\tag{23}
$$

where $\mathrm{E}[\cdot]$ is the expected value operator and S_0 is the power spectral density of the WGN (Crandall and Mark 1963). An analytical solution has been derived for Eq. (23), but its expression is rather cumbersome and thus omitted for the sake of readability. However, Eq. (23) can be easily evaluated by numerical integration. A simple closed-form analytic expression of the expected value of the generated power can be obtained for, both, filtered and pure WGN under the assumption of stationary vibrations as follows

$$
W_\infty = \lim_{T\to\infty}\mathrm{E}[W(T)]
\tag{24}
$$

Specifically, the expected value of the generated power in case of stationary filtered WGN is

$$
\begin{aligned}
W_\infty &\\
= \frac{\pi S_0}{2R}\Bigg\{ &\quad 2r^2CR \\
+ 8rCR&\left(\frac{a_f\left(CR\xi_f\omega_f + 1\right) + b_f CR\widetilde{\omega}_f}{C^2R^2\omega_f^2 + 2C\xi_f R\omega_f + 1} + \frac{a_s(C\xi_s R\omega_s + 1) + b_s CR\widetilde{\omega}_s}{C^2R^2\omega_s^2 + 2CR\xi_s\omega_s + 1}\right) \\
&+ \frac{1}{\xi_f\omega_f}\left(a_f^2\left(1 + \xi_f^2\right) + 2a_f b_f\xi_f\sqrt{1 - \xi_f^2} + b_f^2\left(1 - \xi_f^2\right)\right) \\
&+ \frac{1}{\xi_s\omega_s}\left(a_s^2(1 + \xi_s^2) + 2a_s b_s\xi_s\sqrt{1 - \xi_s^2} + b_s^2(1 - \xi_s^2)\right) \\
+ \frac{8}{\Delta_w}\Big[&\quad a_s a_f\left(\left(\xi_f\omega_f\left((2\xi_s^2 + 1)\omega_s^2 + \omega_f^2\right) + \xi_s\omega_s\left((2\xi_f^2 + 1)\omega_f^2 + \omega_s^2\right)\right)\right) \\
&+ a_s b_f\left(2\xi_f\xi_s\omega_f\omega_s + (2\xi_s^2 - 1)\omega_s^2 + \omega_f^2\right)\widetilde{\omega}_f \\
&+ a_f b_s\left(2\xi_f\xi_s\omega_f\omega_s + \left(2\xi_f^2 - 1\right)\omega_f^2 + \omega_s^2\right)\widetilde{\omega}_s \\
&+ 2b_s b_f\left(\xi_f\omega_f + \xi_s\omega_s\right)\widetilde{\omega}_f\widetilde{\omega}_s\Big]\Bigg\}
\end{aligned}
\tag{25}
$$

where

$$\Delta_w = \omega_f^4 + 4\xi_f\xi_s\omega_f\omega_s\left(\omega_s^2 + \omega_f^2\right) + 2\omega_f^2\omega_s^2\left(2\xi_f^2 + 2\xi_s^2 - 1\right) + \omega_s^4 \tag{26}$$

A more compact analytical expression can be derived for a pure stationary WGN as follows

$$\lim_{\omega_f\to\infty} W_\infty = \frac{\pi\alpha^2\Theta^2\Lambda^2 R S_0}{2\xi_s\omega_s(C^2R^2\omega_s^2 + 2C\xi_s R\omega_s + 1)} \tag{27}$$

The optimal resistive electric load is obtained following the real matching approach (Bechtold *et al.* 2012). Therefore, the optimal resistive electric load $\bar{R}$ and the corresponding optimal generated power $\bar{W}$ can be numerically determined for stationary vibrations as follows

$$\bar{R} = \underset{R}{\operatorname{argmax}}\, W_\infty \tag{28a}$$

$$\bar{W} = \max_R W_\infty \tag{28b}$$

where W_∞ is given by Eq. (25) for stationary filtered WGN whereas its limit value obtained in Eq. (27) must be adopted for a pure stationary WGN.

2.5 Probability of failure of the piezoelectric energy harvester

It is assumed that the failure of the piezoelectric device is due to an excessive value of the displacement response of the piezoelectric strip $y(t)$.

Therefore, the probability of failure of the device can be defined as the probability of the stochastic process $y(t)$ of crossing a symmetric threshold $\pm a$.

Once again, the simplifying assumption of stationary vibrations is adopted, which leads to a conservative reliability assessment of the device.

Under the further hypothesis that the threshold crossing is a rare event, the probability of failure P_f at the time T can be determined as

$$P_f = P_f(\nu_a, T) = 1 - \mathrm{e}^{-\nu_a T} \tag{29}$$

where ν_a is the average rate of crossing of the symmetric threshold, which is given by (Crandall and Mark 1963)

$$\nu_a = \frac{1}{\pi}\frac{\sigma_{\dot{y}}}{\sigma_y}\mathrm{e}^{-\frac{a^2}{2\sigma_y^2}} \tag{30}$$

Herein, $\sigma_{\dot{y}}$ and σ_y are the standard deviations of relative velocity and relative displacement of the harvester, respectively.

For stationary conditions, they are evaluated as follows

$$\sigma_{\dot{y}}^2 = \lim_{T\to\infty} \mathrm{E}[\dot{y}^2(T)] = 2\pi S_0 \lim_{T\to\infty}\int_0^T h_{\dot{y}}^2(t)\mathrm{d}t \tag{31a}$$

$$\sigma_y^2 = \lim_{T\to\infty} \mathrm{E}[y^2(T)] = 2\pi S_0 \lim_{T\to\infty}\int_0^T h_y^2(t)\mathrm{d}t \tag{31b}$$

from which

$$\sigma_{\dot{y}}^2 = \frac{\pi S_0\Lambda^2\alpha^2\omega_f^2\left(\omega_s^2\xi_f^3 + 4\xi_s\omega_s\xi_f^2\omega_f + \xi_f\omega_f^2 + \xi_s\omega_s\omega_f\right)}{2\xi_s\omega_s\xi_f\left(2\omega_s^2\left(2\xi_f^2 + 2\xi_s^2 - 1\right)\omega_f^2 + 4\xi_s\omega_s^3\xi_f\omega_f + 4\xi_s\omega_s\xi_f\omega_f^3 + \omega_f^4 + \omega_s^4\right)} \tag{32a}$$

$$\sigma_y^2 = \frac{\pi S_0\Lambda^2\alpha^2\omega_f\left(4\xi_f\omega_f\left(\xi_f^2 + \xi_s^2\right)\omega_s^2 + 4\xi_s\omega_s\xi_f^2\left(\omega_f^2 + \omega_s^2\right) + \xi_s\omega_s^3 + \xi_f\omega_f^3\right)}{2\xi_s\omega_s^3\xi_f\left(2\omega_s^2\left(2\xi_f^2 + 2\xi_s^2 - 1\right)\omega_f^2 + 4\xi_s\omega_s^3\xi_f\omega_f + 4\xi_s\omega_s\xi_f\omega_f^3 + \omega_f^4 + \omega_s^4\right)} \tag{32b}$$

3. Numerical applications

3.1 Numerical data

Besides piezoelectric energy harvesting from continuous dynamic loads, the possibility of powering wireless micro-sensor networks by scavenging the energy from intermittent dynamic loads is also gaining significant research interest in light of some potential practical applications. The proposed numerical application is concerned with piezoelectric energy harvesting under seismic base accelerations, along the lines of recent numerical and experimental studies that investigated the feasibility of vibrations-powered sensing systems for structural monitoring applications in the event of earthquake, see for instance (Elvin *et al.* 2006, Rhimi and Lajnef 2012, Tomicek *et al.* 2013, Cheng *et al.* 2013, Shen *et al.* 2016, Quaranta *et al.* 2017, 2018).

The piezoelectric strip is assumed to be made of electrospun PVDF nanofibers (Persano *et al.* 2013, 2014, Maruccio and De Lorenzis 2014, Maruccio *et al.* 2015, 2016, Quaranta *et al.* 2018). The material constants adopted for the numerical analyses are the following: $E_m = 1.8\cdot 10^9\ \mathrm{N/m^2}$, $\nu = 0.3$, $d_{31} = 32\cdot 10^{-12}\ \mathrm{m/V}$, $\epsilon_{33}^T = 9\epsilon_0$ (where ϵ_0 is the permittivity of the free space). The electromechanical data are taken from (Persano *et al.* 2013, Ico *et al.* 2016), assuming an average diameter of the fibers equal to 100 nm. The geometry of the strip is $L = 2000\ \mathrm{mm}$, $B = 250$ mm and $H = 0.05\ mm$. These dimensions are compatible with the geometry of similar PVDF-based products available in the market and are consistent with a strip to be inserted within the bounding frame of typical civil structural systems. From Eq. (5), it is thus obtained $C = 7.442\cdot 10^{-7}$ F and $\Theta = 0.0205\ \mathrm{C/m}$.

Two soil conditions are assumed (viz., Case A and Case B), and the numerical values of the corresponding filter parameters are selected among the several proposals collected in (Marano *et al.* 2008). Furthermore, a pure WGN is also considered (viz., Case W) in order to appreciate the influence of the frequency content on the power generated by the harvester. The filter parameters are listed in Table 1.

Case A is representative of a soft soil condition, and it corresponds to a filter period T_{fA} equal to 1.2825 s. Conversely, Case B is representative of a stiff soil condition, and it corresponds to a filter period T_{fB} equal to 0.457 s. Following (Liu *et al.* 2016), S_0 is related to the peak ground acceleration (PGA) $\ddot{x}_b^{max}$ through the following relationship

Table 1 Filter parameters

Parameter	Case A	Case B	Case W
Filter frequency	$\omega_{fA} = 5$ rad/s	$\omega_{fB} = 15$ rad/s	$\omega_{fW} \to \infty$
Filter damping	$\xi_{fA} = 0.20$	$\xi_{fB} = 0.40$	–

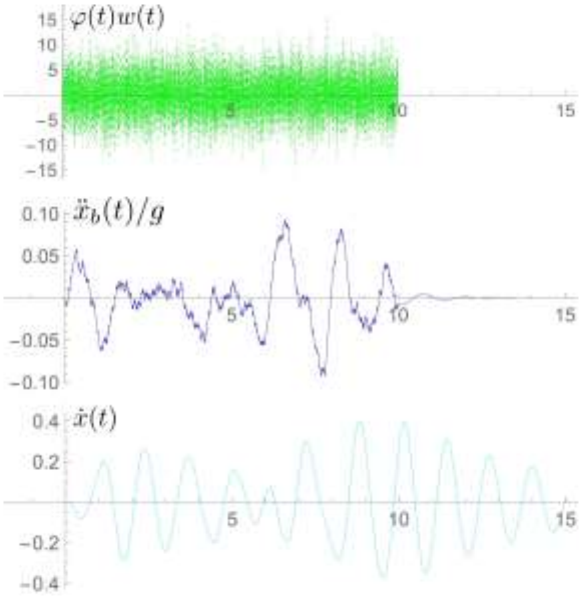

Fig. 5 Thin Sample of the random process $\varphi(t)w(t)$ together with corresponding time histories of $\ddot{x}_b(t)$ and $\dot{x}(t)$

$$S_0 = \frac{(\ddot{x}_b^{max})^2}{\delta^2\left[\pi\omega_f\left(2\xi_f + \frac{1}{2\xi_f}\right)\right]} \tag{33}$$

where the peak factor δ is equal to 2.8. The dimensionless peak ground acceleration $p_b = \ddot{x}_b^{max}/g$ is introduced, where g is the gravity acceleration. Note that the use of Eq. (33) implies that S_0 is proportional to the square value of p_b. In Eq. (33), it will be assumed $p_b = 0.1$. Such a low intensity of the ground motion is selected to focus on frequent seismic events and to fulfill the assumption of linear elastic behavior of the hosting structural system. So doing, S_0 values for Case A and Case B are equal to $S_{0A} = 0.002695\ \mathrm{m}^2/\mathrm{s}^3$ and $S_{0B} = 0.00127065\ \mathrm{m}^2/\mathrm{s}^3$, respectively. The numerical value of S_0 for Case W will be $S_{0W} = S_{0A}$ or $S_{0W} = S_{0B}$ when comparing the corresponding results with that calculated for Case A and Case B, respectively. Here and henceforth, a conventional value of the structural damping $\xi_s = 5\%$ is considered, whereas it is assumed $\alpha = 0.50$ and $\Lambda = 1$ without loss of generality.

With regard to the Case A, Fig. 5 shows a sample of the random process $\varphi(t)w(t)$ together with the corresponding time histories of $\ddot{x}_b(t)$ and $\dot{x}(t)$. The structural circular frequency is assumed in such a way that $T_s = T_{fA} =$ 1.2825 s. In Fig. 5, the continuous stochastic process $w(t)$ has a duration $T = 10$ s. It has been simulated by a discrete sequence of uncorrelated Gaussian variables w_i (with $i = 1, \cdots, 10001$) having zero mean and variance $2\pi S_0/\Delta t$ (Fox *et al.* 1988), where the time step Δt is equal to 0.001 s and S_0 has been determined according to Eq. (33). Note that the obtained peak ground acceleration is close to the target value $p_b = 0.1$.

The following numerical results are shown for a strong-motion duration $T \in [0,10]$ s. The selected values of T_s for the following numerical examples are lower than or equal to the filter period of the soil T_f, i.e. $T_s \in [0,1]T_f$ (where $T_f = T_{fA}$ or $T_f = T_{fB}$ for Case A and Case B, respectively).

The proposed numerical applications are intended to provide an appraisal of the amount of energy that a piezoelectric strip bonded to a framed structural system can generate under frequent and medium-intensity ordinary seismic ground shaking at its base, in such a way to infer whether the considered energy harvesting strategy can be exploited to power a wireless node. Furthermore, the role of hosting structure's dynamics, frequency content of the

3.2 Results

Fig. 6 illustrates the probability of failure P_f as function of the structural period T_s for $T = 10$ s. The dimensionless values of the symmetric threshold $\pm a/L$ are $\pm 1/100$ and $\pm 5/100$ for Case A whereas they are equal to $\pm 1/1000$ and $\pm 5/1000$ for Case B. It is remarked that such probability of failure values are obtained under the simplifying conservative assumption of stationary random vibrations. It can be easily inferred from Fig. 6 that larger stretching values of the piezoelectric strip are achieved for Case A than in Case B mainly because of the lower damping of the filter. While the probability of failure close to resonance conditions (i.e., $T_s \to T_f$) in case of filtered input is equal to or larger than the probability of failure corresponding to a pure WGN, this does not hold always true for low values of the structural period T_s (especially for Case B, which has a greater filter damping value). The results show that the probability of failure always increases with the structural period and, in general, it is strongly influenced by the filter.

The mean value of the generated electric power is depicted in Fig. 7 for three values of the resistive load (i.e., $R = \{10^3, 10^5, 10^7\}\ \Omega$). The resonance condition between the hosting structure and the filter is assumed for, both, Case A and Case B: as a consequence, the electric power generated in Case A or Case B is larger than the value achieved under pure WGN. It can be easily inferred from Fig. 7 that the electric power is not a monotonic function of the resistive load and, as expected, an optimal value of the resistive load exists.

The mean value of the generated electric power is shown in Fig. 8 for $T_s = \{0.2, 0.5, 1.0\}T_f$ (with $R = 10^5\ \Omega$). This figure further highlights the strong influence of the filter's characteristics. The generated power is greater in case of filtered input rather than under pure WGN in

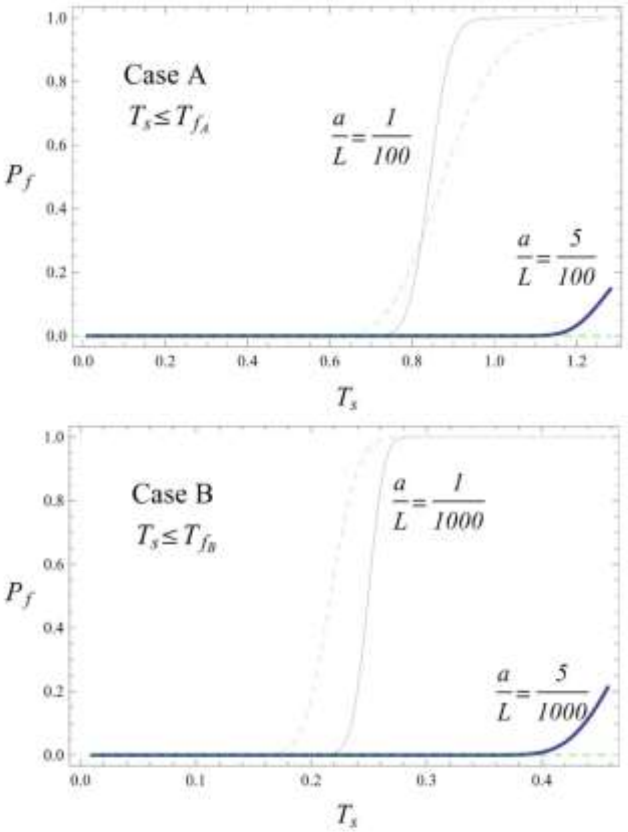

Fig. 6 Probability of failure for different threshold values (continuous lines correspond to Case A in the left picture and to Case B in the right picture whereas dashed lines refer to Case W)

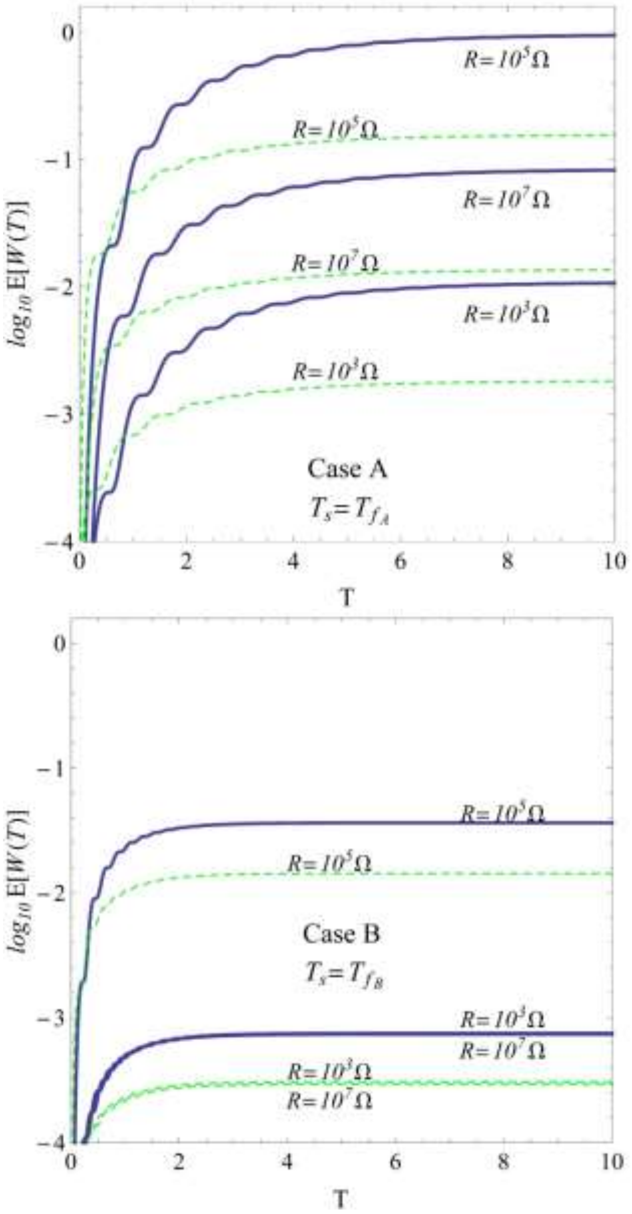

Fig. 7 Mean value of generated electric power for different resistive load values (continuous lines correspond to Case A in the left picture and to Case B in the right picture whereas dashed lines refer to Case W)

resonance conditions (i.e., $T_s = T_{fA}$ for Case A and $T_s = T_{fB}$ for Case B). On the other hand, this is not always true for low values of the structural period T_s (especially for Case B) because of the greater filter damping value.

The optimal values of generated power $\bar{W}$ and resistive electric load $\bar{R}$ under the simplifying hypothesis of stationary random vibrations are given in Fig. 9. Only the results for Case A and Case W are plotted for the sake of conciseness, and they are given as function of the ratio T_s/T_{fA}. These results demonstrate that the frequency content of the random vibrations (i.e., the numerical values of the filter parameters) have a remarkable influence on the optimal value of the resistive electric load. However, it is also worthy to note that the optimal resistive loads corresponding to filtered and pure WGN tend to coincide when the resonance condition is approached.

Finally, the harvested mean power for the optimal value of the electric load resistance $\bar{R} = 10^{5.442}\ \Omega$ corresponding to the resonance condition $T_s = T_{fA}$ (Fig. 9) is shown in Fig. 10 (this value is almost the same in Case A and Case W).

4. Conclusions

An analytical study of electroactive polymeric strips attached to relatively large linear elastic structural systems under random vibrations at the base has been presented.

Specifically, the hosting structure has been reduced to a linear elastic SDOF system whereas the random loading is a filtered WGN, which acts at the base for an arbitrary duration. In agreement with previous analytical studies, a simplified electrical interface consisting of a resistive electrical load is assumed.

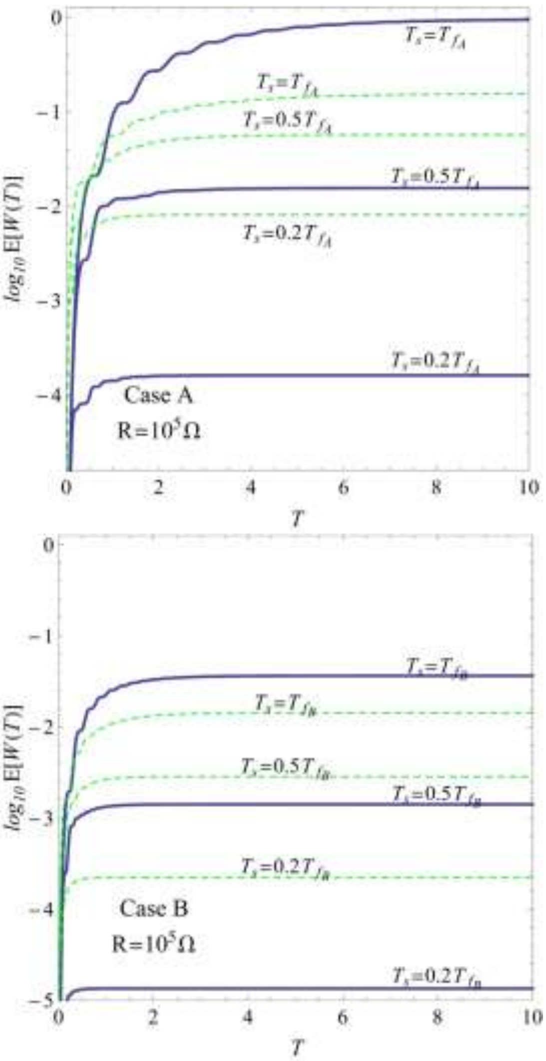

Fig. 8 Mean value of the generated electric power E[W] for different structural periods (continuous lines correspond to Case A in the left picture and to Case B in the right picture whereas dashed lines refers to Case W)

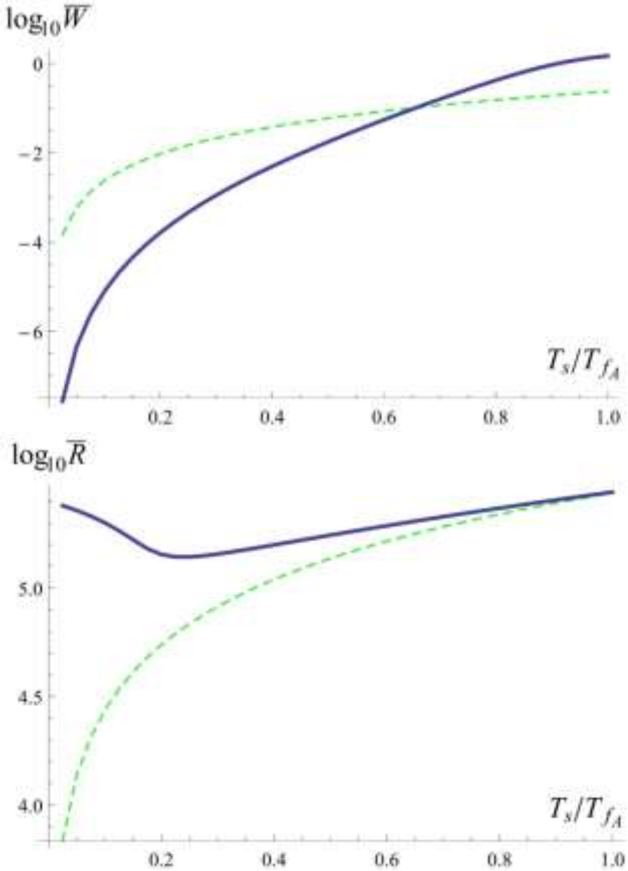

Fig. 9 Optimal value of generated power and optimum resistive electric load (continuous lines correspond to Case A whereas dashed lines refers to Case W)

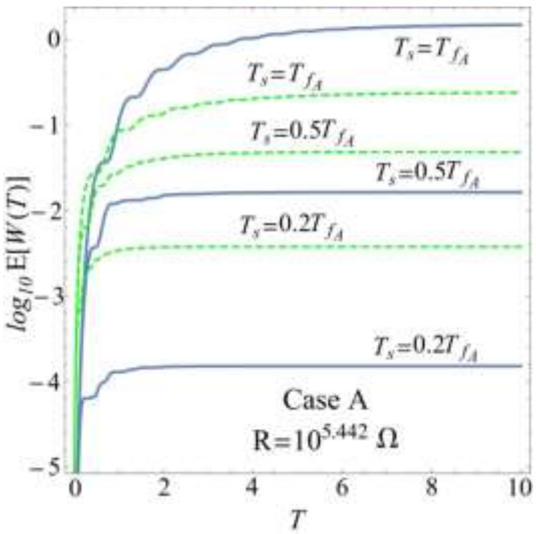

Fig. 10 Mean value of the generated electric power for the optimum resistive electric load (Case A)

The main assumption in the adopted modeling consists in neglecting the electromechanical force with respect to inertial, dissipative and elastic forces exerted on the hosting structure. This assumption is clearly reasonable for applications concerning civil structures. By virtue of this simplified electrodynamic modeling, original compact analytical expressions have been derived in order to estimate the generated electric power and the integrity of the device, thereby facilitating the analysis and design of piezoelectric strips under random vibrations. For the sake of compactness of the final closed-form solutions, a second-order filtering is considered and, as a consequence, the period of the hosting structure is required to be equal to or less than the filter period.

A numerical investigation for an electroactive polymeric strip made of electrospun PVDF nanofibers attached to a frame structure under base accelerations is finally included. The obtained numerical results have highlighted that the frequency content of the random excitation can greatly affect design and final performances. As regards the specific application considered in the numerical investigation, it has been found that the amount of generated electric power even under low seismic excitation levels is quite large and potentially useful in some cases for earthquake-powered wireless nodes. Finally, it is also worthy highlighting that it is straightforward to apply the proposed framework for the analysis and design of some sensing devices made of piezoelectric patches attached to linear elastic systems under random vibrations.

Acknowledgments

Giuseppe Quaranta acknowledges the support from Sapienza University of Rome through the project "Smart solutions for the assessment of structures in seismic areas". Claudio Maruccio acknowledges the support from the Italian MIUR through the project FIRB Futuro in Ricerca 2010 "Structural mechanics models for renewable energy applications" (RBFR107AKG).

References

Adhikari, S., Friswell, M.I. and Inman, D.J. (2009), "Piezoelectric energy harvesting from broadband random vibrations", *Smart Mater. Struct.*, **18**(11), 115005.

Adhikari, S., Friswell, M.I., Litak, G. and Haddad Khodaparast, H. (2016), "Design and analysis of vibration energy harvesters based on peak response statistics", *Smart Mater. Struct.*, **25**(6), 065009.

Ali, S.F., Friswell, M.I. and Adhikari, S. (2011), "Analysis of energy harvesters for highway bridges", *J. Intel. Mat. Syst. Str.*, **22**(16), 1929-1938.

Bechtold, T., Schrag, G. and Feng, L. (2012), *System-level Modeling of MEMS*, John Wiley & Sons.

Cahill, P., Jaksic, V., Keane, J., O'Sullivan, A., Mathewson, A., Ali, S.F. and Pakrashi, V. (2016), "Effect of road surface, vehicle, and device characteristics on energy harvesting from bridge–vehicle interactions", *Comput.-Aided Civil Infrastruct. Eng.*, **31**(12), 921-935. https://doi.org/10.1111/mice.12228.

Cahill, P., Nuallain, N.A.N., Jackson, N., Mathewson, A., Karoumi, R. and Pakrashi, V. (2014), "Energy harvesting from train-induced response in bridges", *J. Bridge Eng.*, **19**(9), 04014034. https://doi.org/10.1061/(ASCE)BE.1943-5592.0000608.

Cahill, P., Pakrashi, V., Sun, P., Mathewson, A. and Nagarajaiah, S. (2018), "Energy harvesting techniques for health monitoring and indicators for control of a damaged pipe structure", *Smart Struct. Syst.*, **21**(3), 287-303. https://doi.org/10.12989/sss.2018.21.3.287.

Cheng, M., Chen, Y., Wei, H. and Seah, W. (2013), "Event-driven energy-harvesting wireless sensor network for structural health monitoring",'*Proceedings of the 2013 IEEE 38th Conference on Local Computer Networks (LCN)*, Sydney (Australia)'.

Crandall, S.H. and Mark, W.D. (1963), *Random Vibration in Mechanical Systems*, Academic Press.

Elvin, N.G., Lajnef, N. and Elvin, A.A. (2006), "Feasibility of structural monitoring with vibration powered sensors", *Smart Mater. Struct.*, **15**(4), 977-986.

Fox, R.F., Gatland, I.R., Roy, R. and Vemuri, G. (1988), "Fast, accurate algorithm for numerical simulation of exponentially correlated colored noise", *Phys. Rev. A*, **38**(11), 5938.

Greco, R. and Trentadue, F. (2013), "Structural reliability sensitivities under nonstationary random vibrations", *Math. Problem. Eng.*, **2013**, 1-31. http://dx.doi.org/10.1155/2013/426361.

Halvorsen, E. (2008), "Energy harvesters driven by broadband random vibrations", *J. Microelectromech. Syst.*, **17**(5), 1061-1071. DOI: 10.1109/JMEMS.2008.928709.

Hancke, G.P., de Carvalho e Silva, B. and Hancke, G.P. (2013), "The role of advanced sensing in smart cities", *Sensors*, **13**(1), 393-425. https://doi.org/10.3390/s130100393.

He, Q. and Daqaq, M.F. (2016), "Electric load optimization of a nonlinear mono-stable Duffing harvester excited by white noise", *Meccanica*, **51**(5), 1027-1039.

Ico, G., Showalter, A., Bosze, W., Gott, S.C., Kim, B.S., Rao, M.P., Myung, N.V. and Nam, J. (2016), "Size-dependent piezoelectric and mechanical properties of electrospun P(VDF-TrFE) nanofibers for enhanced energy harvesting", *J. Mater. Chemistry A*, **4**, 2293-2304.

Karimi, M., Tikani, R., Ziaei-Rad, S. and Mirdamadi, H. (2016), "Experimental and theoretical studies on piezoelectric energy harvesting from low-frequency ambient random vibrations", *Proceedings of the Institution of Mechanical Engineers, Part C: Journal of Mechanical Engineering Science* **230**(14), 2363-2375.

Kefal, A., Maruccio, C., Quaranta, G. and Oterkus, E. (2019), "Modelling and parameter identification of electromechanical systems for energy harvesting and sensing", *Mech. Syst. Signal Pr.*, **121**, 890-912. https://doi.org/10.1016/j.ymssp.2018.10.042.

Liu, Z., Liu, W. and Peng, Y. (2016), "Random function based spectral representation of stationary and nonstationary stochastic processes", *Probabilist Eng. Mech.*, **45**, 115-126. https://doi.org/10.1016/j.probengmech.2016.04.004.

Marano, G., Morrone, E. and Quaranta, G. (2009), "Analysis of randomly vibrating structures under hybrid uncertainty", *Eng. Struct.*, **31**(11), 2677-2686. https://doi.org/10.1016/j.engstruct.2009.06.016.

Marano, G., Trentadue, F., Morrone, E. and Amara, L. (2008), "Sensitivity analysis of optimum stochastic nonstationary response spectra under uncertain soil parameters", *Soil Dynam. Earthq. Eng.*, **28**(12), 1078-1093. https://doi.org/10.1016/j.soildyn.2007.12.003.

Maruccio, C. and De Lorenzis, L. (2014), "Numerical homogenization of piezoelectric textiles for energy harvesting", *Fract. Struct. Integrity*, **1**(29), 49-60.

Maruccio, C., De Lorenzis, L., Persano, L. and Pisignano, D. (2015), "Computational homogenization of fibrous piezoelectric materials", *Comput. Mech.*, **55**(5), 983-998.

Maruccio, C., Quaranta, G., De Lorenzis, L. and Monti, G. (2016), "Energy harvesting from electrospun piezoelectric nanofibers for structural health monitoring of a cable-stayed bridge", *Smart Mater. Struct.*, **25**(8), 085040.

Maruccio, C., Quaranta, G., Montegiglio, P., Trentadue, F. and Acciani, G. (2018), "A two-step hybrid approach for modeling the nonlinear dynamic response of piezoelectric energy harvesters", *Shock Vib.*, **2018**. https://doi.org/10.1155/2018/2054873.

Peigney, M. and Siegert, D. (2013), "Piezoelectric energy harvesting from traffic-induced bridge vibrations", *Smart Mater. Struct.*, **22**(9), 1-11.

Persano, L., Dagdeviren, C., Maruccio, C., De Lorenzis, L. and Pisignano, D. (2014), "Cooperativity in the enhanced piezoelectric response of polymer nanowires", *Adv. Mater.*,

26(45), 7574-7580. https://doi.org/10.1002/adma.201403169.
Persano, L., Dagdeviren, C., Su, Y., Zhang, Y., Girardo, S., Pisignano, D., Huang, Y. and Rogers, J. (2013), "High performance piezoelectric devices based on aligned arrays of nanofibers of PVDF", *Nature Commun.*, **1633**, 1-4.
Quaranta, G., Trentadue, F., Maruccio, C. and Marano, G. (2017), "Energy harvesting from earthquake for vibration-powered wireless sensors", *Proceedings of the 4th Conference on Smart Monitoring, Assessment and Rehabilitation of Structures (SMAR 2017)*, Zürich (Switzerland)".
Quaranta, G., Trentadue, F., Maruccio, C. and Marano, G. (2018), "Analysis of piezoelectric energy harvester under modulated and filtered white Gaussian noise", *Mech. Syst. Signal Pr.*, **104**, 134-144. https://doi.org/10.1016/j.ymssp.2017.10.031.
Rhimi, M. and Lajnef, N. (2012), "Tunable energy harvesting from ambient vibrations in civil structures", *J. Energy Eng.*, **138**(4), 185-193. https://doi.org/10.1061/(ASCE)EY.1943-7897.0000077.
Roberts, J. B. and Spanos, P. (1990), *Random vibration and statistical linearization*, John Wiley and Sons.
Shen, W., Zhu, S., Zhu, H. and Xu, Y. (2016), "Electromagnetic energy harvesting from structural vibrations during earthquakes", *Smart Struct. Syst.*, **18**(3), 449-470. http://dx.doi.org/10.12989/sss.2016.18.3.449.
Tomicek, D., Tham, Y., Seah, W. and Rayudu, R. (2013), "Vibration-powered wireless sensor for structural monitoring during earthquakes", *Proceedings of the 6th International Conference on Structural Health Monitoring of Intelligent Infrastructure (SHMII-6 2013)*, Hong Kong (P.R. China)".
Xiao, H., Wang, X. and John, S. (2015), "A dimensionless analysis of a 2DOF piezoelectric vibration energy harvester", *Mech. Syst. Signal Pr.*, **58-59**, 355-375.
Xie, X., Wang, Q. and Wang, S. (2015), "Energy harvesting from high-rise buildings by a piezoelectric harvester device", *Energy* **93**, 1345-1352.
Xie, X., Wu, N., Yuen, K. and Wang, Q. (2013), "Energy harvesting from high-rise buildings by a piezoelectric coupled cantilever with a proof mass", *Int. J. Eng. Sci.*, **72**, 98-106. https://doi.org/10.1016/j.ijengsci.2013.07.004.
Yang, Z., Erturk, A. and Zu, J. (2017), "On the efficiency of piezoelectric energy harvesters", *Extreme Mech. Lett.*, **15**, 26-37. https://doi.org/10.1016/j.eml.2017.05.002.
Zhang, Y., Cai, S.C.S. and Deng, L. (2014), "Piezoelectric-based energy harvesting in bridge systems", *J. Intel. Mat. Syst. Str.*, **25**(12), 1414-1428. https://doi.org/10.1177/1045389X13507354.
Zhao, S. and Erturk, A. (2012), "Electroelastic modeling and experimental validations of piezoelectric energy harvesting from broadband random vibrations of cantilevered bimorphs", *Smart Mater. Struct.*, **22**(1), 015002.

HJ